SUPPLEMENTARY FIGURES

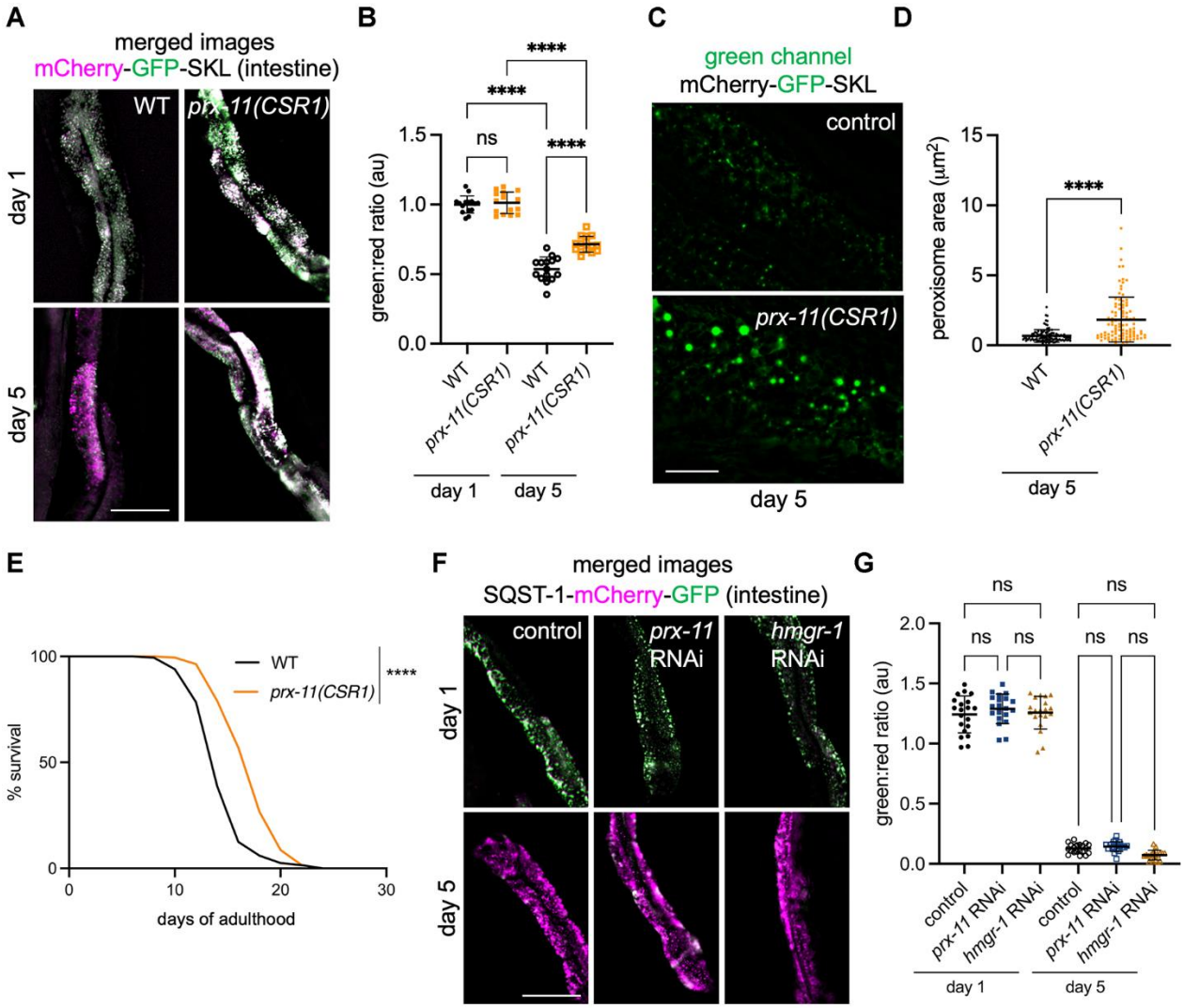

Supplementary Figure 1. Loss of *prx-11* function, such as in *prx-11(CSR1)* mutants, is associated with peroxisome enlargement, lifespan extension, and a reduction in pexophagy but not autophagy in general. (**A**) Representative merged green and red fluorescence images of the mCherry-GFP-SKL pexophagy reporter at day 1 and day 5 of adulthood in wild-type and *prx-11(CSR1)* animals. Pexophagy is indicated by a decrease in green fluorescence, which is sensitive to acidic pH, relative to red fluorescence, which is insensitive to acidic pH. (**B**) Quantification of green:red fluorescence ratios for mCherry-GFP-SKL at day 1 and day 5 of adulthood in wild-type and *prx-11(CSR1)* animals (n = 20 worms per condition). Data are presented as mean ± SD. ****, $p \leq 0.0001$; ns, not significant. One-way ANOVA with Tukey's multiple comparisons. (**C**) Representative green channel images of mCherry-GFP-SKL at day 5 of adulthood in wild-type and *prx-11(CSR1)* animals. (**D**) Quantification of individual peroxisome areas at day 5 of adulthood in wild-type and *prx-11(CSR1)* animals. Data are presented as mean ± SD. ****, $p \leq 0.0001$. Unpaired t-test. (**E**) Lifespan analysis of wild-type and *prx-11(CSR1)* animals. Wild-type: Mean lifespan = 14.66 days, n = 199 worms. *prx-11(CSR1)*: Mean lifespan = 17.37 days, n = 195 worms. Significance was determined using a log-rank test. Wild-type vs. *prx-11(CSR1)*: $X^2 = 79.33$, $p \leq 0.0001$. (**F**) Representative merged green and red fluorescence images of the SQST-1-mCherry-GFP autophagy reporter at day 1 and day 5 of adulthood in animals fed either control, *prx-11,* or *hmgr-1* RNAi. Autophagic activity is indicated by a decrease in green fluorescence, which is sensitive to acidic pH, relative to red fluorescence, which is insensitive to acidic pH. (**G**) Quantification of green:red fluorescence ratios for SQST-1-mCherry-GFP at day 1 and day 5 of adulthood in animals fed either control, *prx-11,* or *hmgr-1* RNAi (n = 20 worms per condition). Data are presented as mean ± SD. ns, not significant. One-way ANOVA with Tukey's multiple comparisons. Bars: 10 μm (**C**) or 100 μm (**A**, **F**).

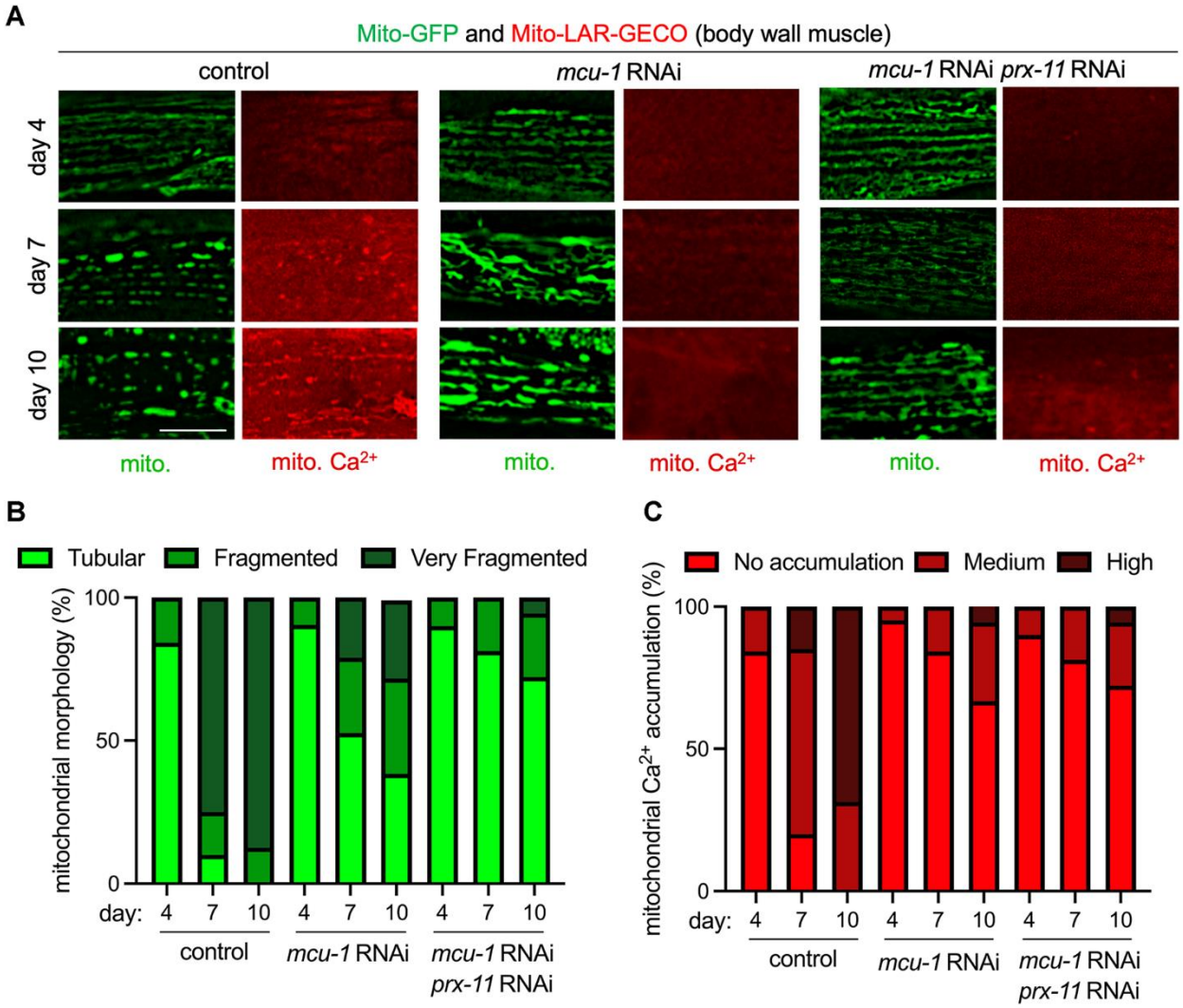

Supplementary Figure 2. *mcu-1* knockdown suppresses age-dependent mitochondrial Ca^{2+} accumulation and, partly, mitochondrial fragmentation. (**A**) Representative images of Mito-GFP and the Mito-LAR-GECO Ca^{2+} reporter in body wall muscle of day 4, day 7, and day 10 adult hermaphrodite animals fed either control RNAi alone, *mcu-1* RNAi alone, or *mcu-1* RNAi in combination with *prx-11* RNAi. (**B**, **C**) Classification of mitochondrial morphology and mitochondrial Ca^{2+} accumulation in day 4, day 7, and day 10 adult hermaphrodite animals fed either control RNAi alone, *mcu-1* RNAi alone, or *mcu-1* RNAi in combination with *prx-11* RNAi. Bar: 10 µm.

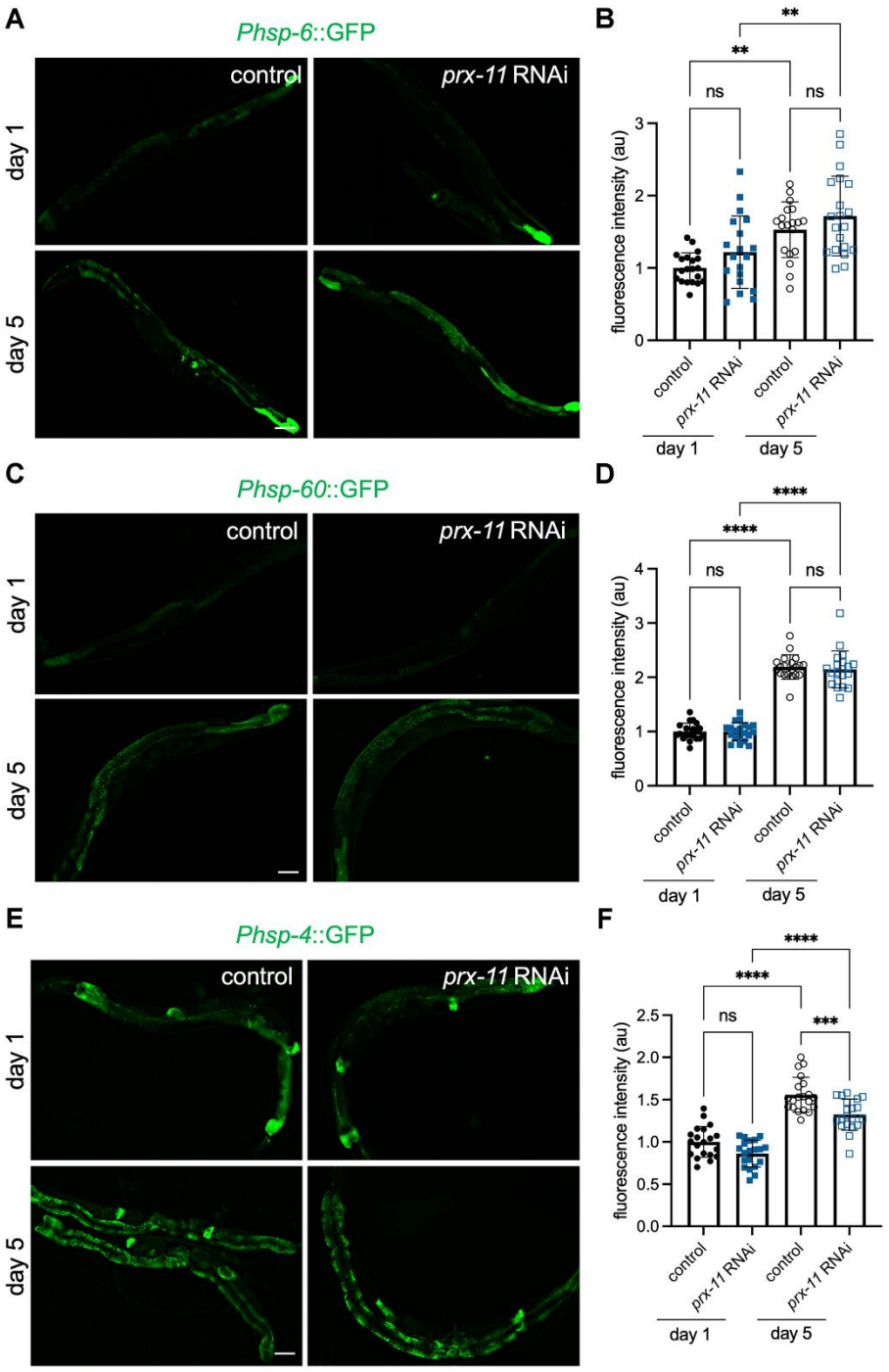

Supplementary Figure 3. *prx-11* RNAi does not activate mitochondrial or endoplasmic reticulum unfolded protein responses. (**A**) Representative images of *Phsp-6*::GFP in day 1 and day 5 adult hermaphrodite animals fed either control or *prx-11* RNAi. (**B**) Quantification of *Phsp-6*::GFP fluorescence intensities in day 1 and day 5 adult hermaphrodite animals fed either control or *prx-11* RNAi (n = 20 worms per condition). Data are presented as mean ± SD. **, $p \leq 0.01$; ns, not significant. One-way ANOVA with Tukey's multiple comparisons. (**C**) Representative images of *Phsp-60*::GFP in day 1 and day 5 adult hermaphrodite animals fed either control or *prx-11* RNAi. (**D**) Quantification of *Phsp-60*::GFP fluorescence intensities in day 1 and day 5 adult hermaphrodite animals fed either control or *prx-11* RNAi (n = 20 worms per condition). Data are presented as mean ± SD. ****, $p \leq 0.0001$; ns, not significant. One-way ANOVA with Tukey's multiple comparisons. (**E**) Representative images of *Phsp-4*::GFP in day 1 and day 5 adult hermaphrodite animals fed either control or *prx-11* RNAi. (**F**) Quantification of *Phsp-4*::GFP fluorescence intensities in day 1 and day 5 adult hermaphrodite animals fed either control or *prx-11* RNAi (n = 20 worms per condition). Data are presented as mean ± SD. ****, $p \leq 0.0001$; ***, $p \leq 0.001$; ns, not significant. One-way ANOVA with Tukey's multiple comparisons. Bars: 100 µm.

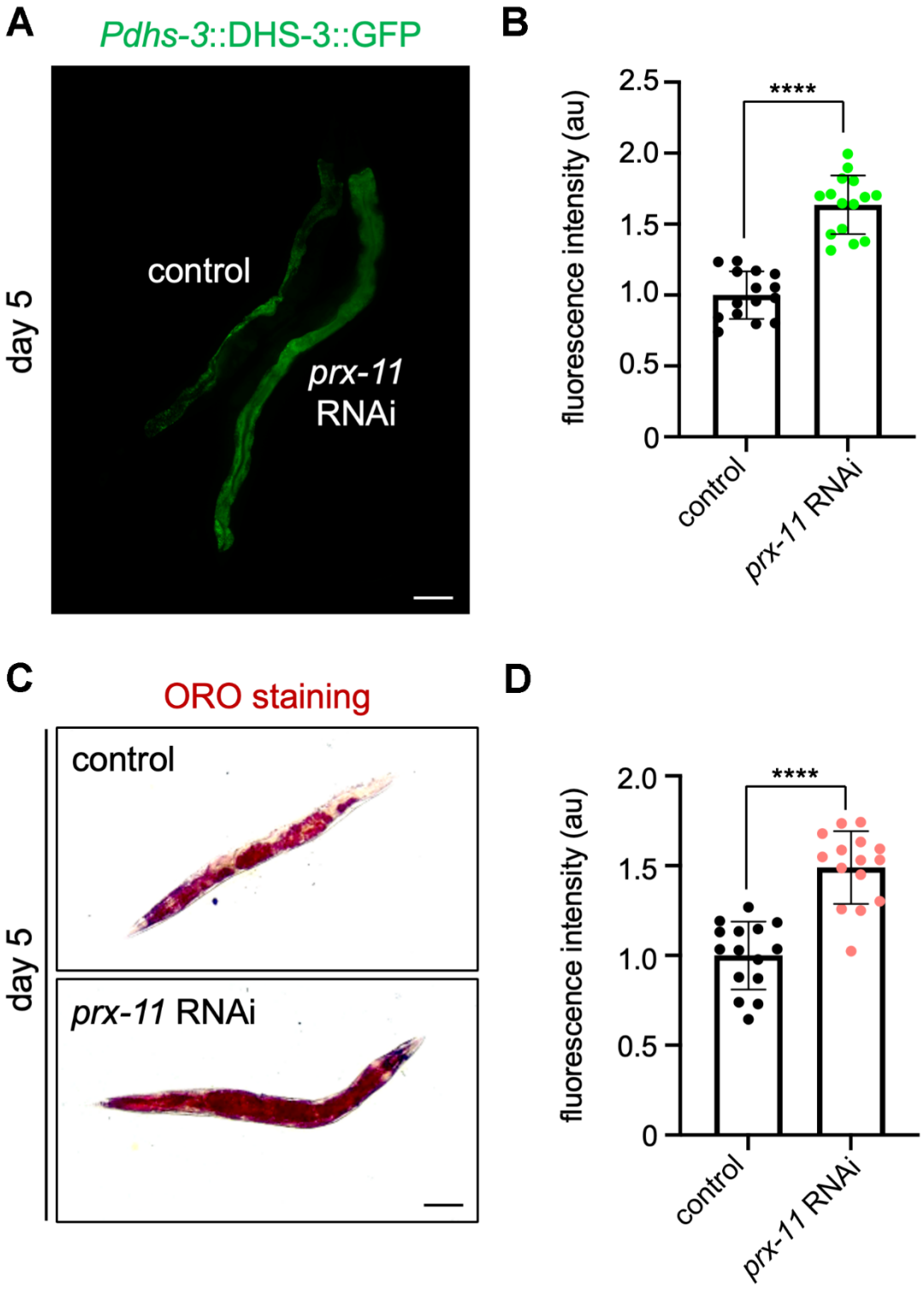

Supplementary Figure 4. *prx-11*-RNAi animals have increased lipid content. (**A**) Representative image of *Pdhs-3*::DHS-3::GFP fluorescence in day 5 adult hermaphrodite animals fed either control or *prx-11* RNAi. (**B**) Quantification of *Pdhs-3*::DHS-3::GFP fluorescence intensities in day 5 adult hermaphrodite animals fed either control or *prx-11* RNAi (n = 15 worms per condition). Data are presented as mean ± SD. ****, $p \leq 0.0001$. Unpaired t-test. (**C**) Representative images of ORO-stained day 5 adult hermaphrodite animals fed either control or *prx-11* RNAi. (**D**) Quantification of ORO staining fluorescence intensities in day 5 adult hermaphrodite animals fed either control or *prx-11* RNAi (n = 15 worms per condition). Data are presented as mean ± SD. ****, $p \leq 0.0001$. Unpaired t-test. Bars: 100 µm.

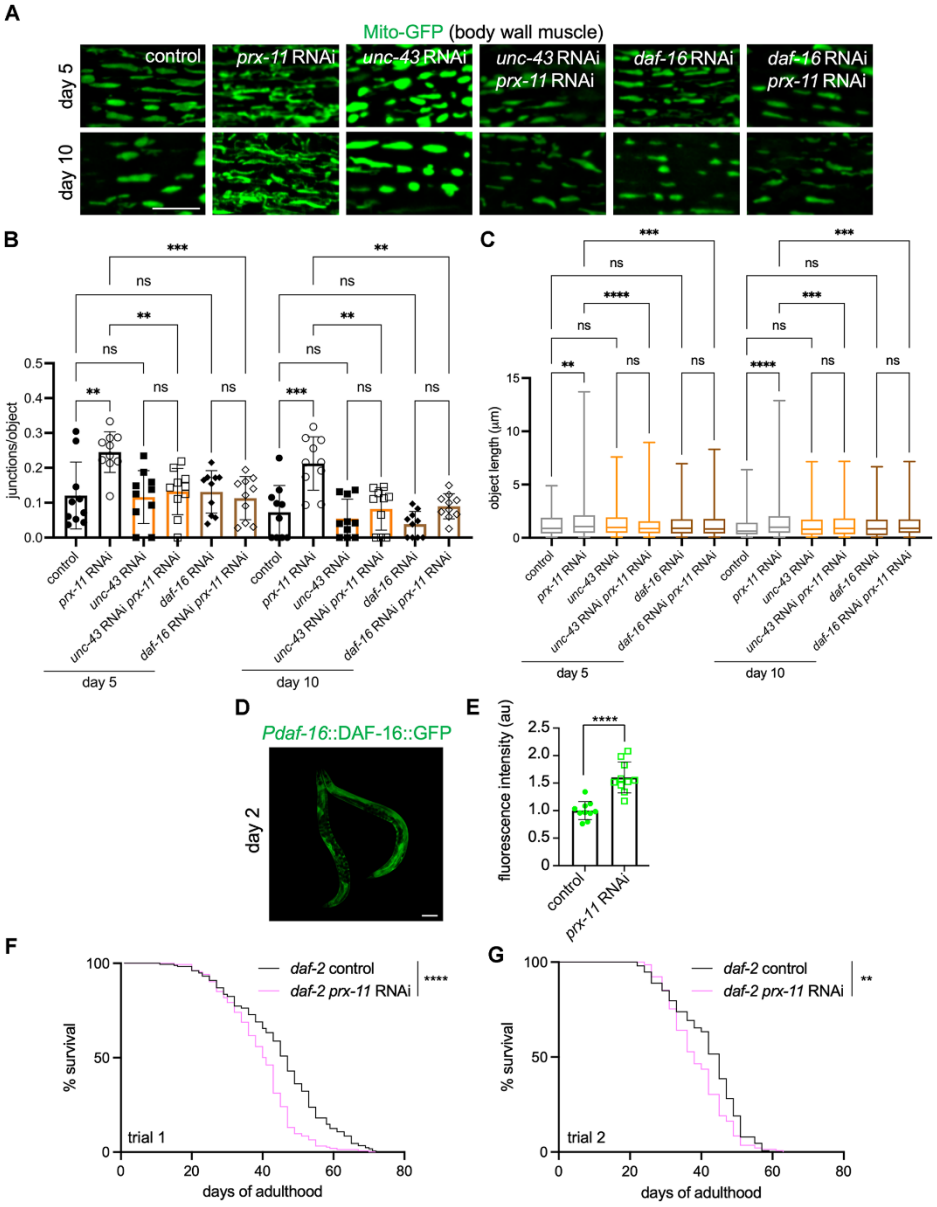

Supplementary Figure 5. Mitochondrial tubulation during aging in *prx-11*-RNAi animals requires *daf-16* and *unc-43*. (**A**) Representative images of Mito-GFP in body wall muscles of day 5 and day 10 adult hermaphrodite animals fed either control RNAi alone, *prx-11* RNAi alone, *unc-43* RNAi alone, *unc-43* and *prx-11* RNAi in combination, *daf-16* RNAi alone, or *daf-16* and *prx-11* RNAi in combination. (**B**) Quantification of mitochondrial junctions per object in day 5 and day 10 adult hermaphrodite animals fed either control RNAi alone, *prx-11* RNAi alone, *unc-43* RNAi alone, *unc-43* and *prx-11* RNAi in combination, *daf-16* RNAi alone, or *daf-16* and *prx-11* RNAi in combination (n = 10 worms per condition). Data are presented as mean ± SD. ***, $p \leq 0.001$; **, $p \leq 0.01$; ns, not significant. One-way ANOVA with Tukey's multiple comparisons. (**C**) Mito-GFP object lengths in day 5 and day 10 adult hermaphrodite animals fed either control RNAi alone, *prx-11* RNAi alone, *unc-43* RNAi alone, *unc-43* and *prx-11* RNAi in combination, *daf-16* RNAi alone, or *daf-16* and *prx-11* RNAi in combination (n = 10 worms per condition). Data are presented as box-and-whisker plots (minimum, 25th percentile, median, 75th percentile, maximum). ****, $p \leq 0.0001$; ***, $p \leq 0.001$; **, $p \leq 0.01$; ns, not significant. One-way ANOVA with Tukey's multiple comparisons. (**D**) Representative image of *Pdaf-16*::DAF-16::GFP fluorescence in day 2 adult hermaphrodite animals fed either control or *prx-11* RNAi. (**E**) Quantification of *Pdaf-16*::DAF-16::GFP fluorescence intensities in day 2 adult hermaphrodite animals fed either control or *prx-11* RNAi (n = 10 worms per condition). Data are presented as mean ± SD. ****, $p \leq 0.0001$. Unpaired t-test. (**F**) Trial 1 lifespan analysis of *daf-2* hermaphrodite animals fed either control or *prx-11* RNAi. *daf-2* control: Mean lifespan = 44.93 days, n = 177 worms. *daf-2 prx-11* RNAi: Mean lifespan = 39.38 days, n = 154 worms. Significance was determined using a log-rank test. *daf-2* control vs. *daf-2 prx-11* RNAi: $X^2 = 30.41$, $p \leq 0.0001$. (**G**) Trial 2 lifespan analysis of *daf-2* hermaphrodite animals fed either control or *prx-11* RNAi. *daf-2* control: Mean lifespan = 41.67 days, n = 153 worms. *daf-2 prx-11* RNAi: Mean lifespan = 38.77 days, n = 142 worms. Significance was determined using a log-rank test. *daf-2* control vs. *daf-2 prx-11* RNAi: $X^2 = 9.69$, $p \leq 0.01$. Bars: 10 µm (**A**) or 100 µm (**D**).